-RESEARCH PAPER-

International Journal of Mining and Geo-Engineering

IJMGE

IJMGE 60-1 (2026) 67-74

DOI: 10.22059/IJMGE.2026.402941.595307

Structural study of the crust from gravity data: case of the Babouri-Figuil and Mayo Oulo-Lere basins (Central Africa)

Saidou Bouba [a], Nlen wounle Barnabas Yaya [a, *], Salomon Nguilaye [a], Bouba Apollinaire [b], Oyoa Valentin [c] and Mohamadou Alidou [a]

[a] *Department of Physics, University of Maroua, Maroua, Cameroon.*

[b] *Department of Physics, University of Garoua, Garoua, Cameroon.*

[c] *Department of Physics, University of Bertoua, Bertoua, Cameroon.*

Article History:

Received: 25 September 2025.

Revised: 29 November 2025.

Accepted: 17 February 2026.

ABSTRACT

This study aimed to extract the lineaments in the crust of the sedimentary basins of Babouri-Figuil and Mayo Oulo-Lere, (Central Africa) from combined terrestrial and EGM2008 model gravity data. For this, data processing and edge detections were completed using filters. The MGTHG (Modified Gudermannian function) filter was applied because of its accuracy in detecting lateral boundaries of the causative structures. This approach has allowed establishing a new structural map of the study area. This map shows several lineaments detected in the region oriented in the WSW-ENE, NE-SW, E-W and NNW-SSE directions. A comparison of this map with those established in previous studies using other filters shows that in addition to the already existing lineaments, new ones have been detected. This proves that the MGTHG filter produces good results in the region. The results of this study provide new insights in the region's tectonic framework.

Keywords: *Gravity data, MGTHG filter, Sedimentary basins, Structural map.*

1. Introduction

Edge detection methods of magnetic and gravity sources play a very important role in the interpretation of geological structures of the subsoil [1, 2]. One of the applications of these methods consists in revealing the probable locations of geological contacts, faults or other tectonic characteristics using various filters [3]. These methods are widely used in mineral exploration, oil and gas prospecting, and environmental studies, which provide crucial information on the complexities of the subsurface [27]. Several edge detection filters have been developed and improved to obtain better solutions for detecting edges of geological structures from potential field data. Most of these filters are based on vertical and horizontal derivatives of the field or their combination [2, 4-7]. The total horizontal gradient (THG) which produce maximum values located above the limits of the sources was used [8]. It was suggested [9], using the maximum values of the amplitude of the analytical signal (AS) to delimit the lateral limits. Another method, based on the THG of a sum of vertical gradients of an increasing order, was introduced by [10] to improve the edge detection results. The disadvantage of the methods based on derivatives is their low resolution and their low performance to balance the amplitudes of anomalies produced by responsible sources located at different depths simultaneously [5, 11]. To overcome these limits, others methods of edge detections have been developed for a more precise delimitation of the geological characteristics that could be hidden [1, 12, 13]. It was introduced by [14], the tilt angle method (TA) that uses the amplitude of the total horizontal derivative to normalize the vertical derivative. A detector of the edges based on the amplitude of the gradient of the tilt derivative was suggested [15]. It was introduced the normalized gradient amplitude technique [16]. These edge detection methods are frequently used in the interpretation of anomalies to delineate geological structures. However, they often face several challenges, including low resolution, which can obscure structural details and thus lead to misinterpretation. Moreover, these methods often generate false outlines, which can create misleading artifacts in the data and further complicate the interpretation process. They often depend on depth data which can introduce inaccuracies, particularly in areas with complex geology [27]. These problems require more advanced filtering methods capable of providing higher resolution, minimizing false edges, and enabling reliable edge detection without relying on depth data. Therefore, in recent years, several other methods using new filters have been developed [17-27] with the aim of improving the accuracy and reliability in edge detection, thus enabling better data analysis in geological studies. Thus, in this work, the Modified Gudermannian Function (MGTHG) method developed by [27] and offering satisfactory results was applied to the gravity data of the Babouri-Figuil and Mayo Oulo-Léré area, a geologically complex region in order to extract the lineaments of the crust of this area. The effectiveness and relevance of this method was demonstrated by [27] after applying it first to a synthetic density model and then to real data from the Georgia area in the United States.

2. Geological and tectonic setting

The North Cameroon has intracratonic sedimentary basins born from the opening of the South Atlantic to the lower Cretaceous. The Babouri-

* Corresponding author. *Tel.*: +237694930704, *E-mail address:* nlenbarna@gmail.com (N. W. B. Yaya).

Figuil and Mayo Oulo basins are part of it. Several previous studies have been carried out there and describe them as synclines characterized by synsedimentary deposits. The Babouri-Figuil and Mayo Oulo Basins are small sedimentary basins elongated in the E-W direction. They are respectively located between latitudes 9°44'- 9°50 'and 9°39'- 9°44' and longitudes 13°44'- 14°02 'and 13°43'- 14°28' (Figure 1). These two basins represent equivalents of the Wealdian facies (lower Cretaceous) of the formation of Bima in Nigeria [28]. The Babouri-Figuil sedimentary basin is the most northern of the small cretaceous basins with continental sediment from northern Cameroon. It measures almost 45 km long and reached 1 km wide line [28, 29]. It is dotted with hillocks and basal sandstone. Its sedimentary pile locally reaches 1500 m. These sediments are constituted of fine sandstones, siltstones and marls. Their presence testifies to sedimentation under a shallow water layer which originates from the indicators of numerous phases of emergence. The abundance of flora as well as the existence of several evaporate levels (gypsum) are present throughout the basin. The marshy environment in a hot and humid climate is revealed by the abundance of Estheries, the dissemination of whose eggs is favored by periods of seasonal drying. More or less charcoal-covered leafy twig prints and dinosaur footprints have been found in Mayo-Tafal. The Mayo Oulo-Lere basin is more than 50 km long and less than 10 km wide. It extends towards the South of Chad, where part of the name "Lere" comes from. It is separated from the Babouri-Figuil basin by granito-gneissic complexes culminating at around 800 m (Figure 2). It is mainly made up of hardened silts and clays. According to the study of the paleoflora, the sedimentary basin of Mayo Oulo-Lere is composed of small graben [28, 30]. These grabens, developed in an extensive north-south oriented context, are made up of basaltic formations [31]. Microfossils collected in this basin are attributed to pre-Aptian sedimentation. From a tectonic point of view, the Babouri-Figuil and Mayo Oulo-Lere basins have undergone intense volcanic activity, leading to the appearance of volcanic materials on the surface through deep fractures. These basins are associated with the Cameroon Volcanic Line (CLV). This major tectonic structure is a Y-shaped chain of intra-plate volcanoes that extends from Pagalu Island in the Atlantic Ocean to western Africa for about 2000 km [32]. The first branch corresponds to the Benue Trough in Cameroon, called the Yola-Garoua basin, while the Babouri-Figuil and Mayo Oulo-Lere basins are connected and the second branch is located in Nigeria. The volcanic rocks along this general line are mainly composed of basalts. Their topographic expressions are accompanied by fissures, fractures, lavas, and tuffs.

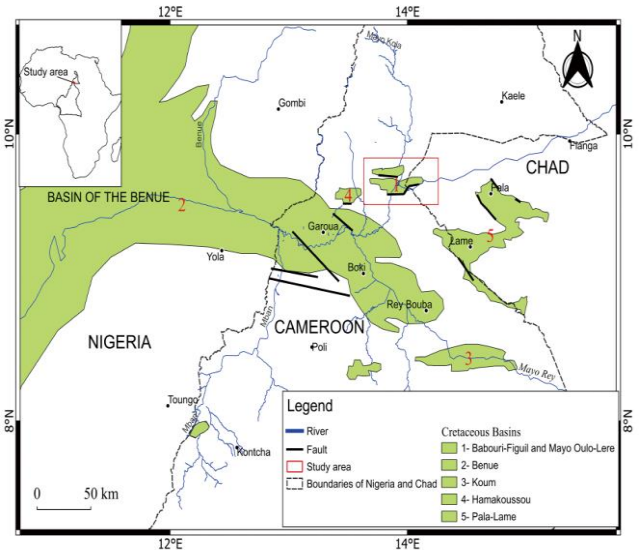

Figure 1. Location map of the Babouri-Figuil and Mayo Oulo-Lere sedimentary basins modified from [33].

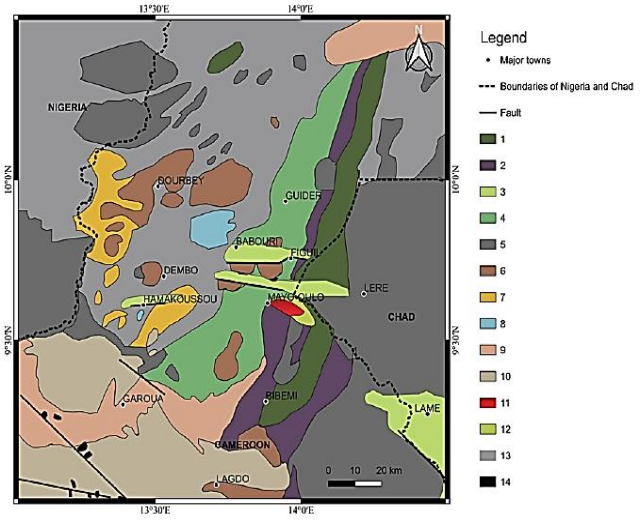

Figure 2: Geological map of the study area (modified from [34, 35]. 1: Mica schist. 2: Lower gneiss. 3: Sedimentary formations. 4: Embrechites Migmatite. 5: Old syn-tectonic granitoid. 6: Late syn–tectonic granitoid. 7: Anatexites granitoid. 8: Post–tectonic granitoid. 9: Quaternary alluvium. 10: Cretaceous Benue Sandstone. 11: Plio–Pleistocene sediments. 12: Conglomerates (sandstone and lavas). 13: Anatexites Migmatite. 14: Basalt.

3. Data and methods

3.1. Data

Gravity database (3116 data) used in this work is obtained by combining terrestrial and EGM2008 data. [36-39] showed the proximity between these two databases of the study area and concluded that they can be combined in order to have a densified database and which will contain more information.

- ***Terrestrial gravity data***

The 515 terrestrial gravity data used in this work were collected between 1960 and 1968 during geophysical reconnaissance campaigns in Central Africa by the Office de Recherche Scientifique et Technique d'Outre–mer (ORSTOM) [40, 41] and completed by Hedberg, ELF (Essences et Lubrifiants de France), the University of Leeds and the IRGM (Institut de Recherche Géologique et Minière) [42]. These data acquisition campaigns were carried out by car, along roads, crossable tracks, and sometimes water courses. Measurements were taken approximately every 3 km. Several gravimeters (Worden and Lacoste & Romberg) were used. The precision of the gravity values is in the order of 0.2 mGal. The location of the measuring stations was determined on topographic maps. Altitudes were estimated using barometers and altimeters (Wallace and Thierman, Thommen). The free air and the plate correction were computed assuming a mean crustal density of 2.67 g/cm^3.

- ***Data from the EGM2008 model***

In this study, we also used gravity data acquired from the Earth Gravitational Model 2008 (EGM2008) via the Bureau Gravimétrie International (BGI). Several works have demonstrated the effectiveness and relevance of gravity data derived from this model in geological and geophysical explorations particularly in our study area [36, 37, 43, 44]. This model is completed to degree and order 2159, and contains additional coefficients up to degree 2190 and order 2159 [45]. It provides gravity data with a spatial resolution of 5 minutes of arc. It integrates land, airborne and maritime gravity data as well as satellite altimetry-derived data. For this study, 2601 data from this model were used.

3.2. Methods

There are several commonly used filters to detect the geological structures edges (deep and shallow) we have:

- ***Total horizontal gradient (THG)***

THG is a filter used to identify the horizontal boundaries of potential field sources. According to [8] these limits correspond to the highest values of the field. THG can be expressed as follows:

$$THG = \sqrt{\left(\frac{\partial F}{\partial x}\right)^2 + \left(\frac{\partial F}{\partial y}\right)^2} \quad (1)$$

where $\frac{\partial F}{\partial x}$ and $\frac{\partial F}{\partial y}$ represent the partial derivatives of the field F in the x and y directions.

- ***Analytical Signal (AS)***

The AS also called total gradient is one of the most used filters introduced by [9]. The maximum values of the amplitude of the analytical signal on the grid plane are used to detect the lateral boundaries of abnormal bodies. The AS is defined as follows:

$$AS = \sqrt{\left(\frac{\partial F}{\partial x}\right)^2 + \left(\frac{\partial F}{\partial y}\right)^2 + \left(\frac{\partial F}{\partial z}\right)^2} \quad (2)$$

where $\frac{\partial F}{\partial z}$ represents the partial derivative of the field F in the z direction.

The ability of THG and AS methods to delineate deep source edges is very limited [46-50].

- ***Tilt angle (TA)***

The TA is a filter that normalizes the vertical derivative using the horizontal derivatives. It can be expressed as follows [14]:

$$TA = tan^{-1}\left(\frac{\frac{\partial F}{\partial z}}{THG}\right) \quad (3)$$

It was showed that field amplitude does not provide distinct signals beyond horizontal limits although it can detect anomalies at different depths [3].

- ***Total horizontal gradient of tilt angle (THGTA)***

It was demonstrated that the total horizontal gradient of tilt angle is more effective and accurate in delineating horizontal boundaries than THG and TA [15]. The amplitude of the THGTA is expressed as follows:

$$THGTA = \sqrt{\left(\frac{\partial TA}{\partial x}\right)^2 + \left(\frac{\partial TA}{\partial y}\right)^2} \quad (4)$$

However, as the source depth increases, the amplitude of the transformed signal decreases [51].

- ***Improved tilt angle (TDX)***

It was presented an improved version of the TA, called the normalized total horizontal gradient (TDX) filter [16]. This filter normalizes the THG using the vertical gradient and identifies maxima along the horizontal boundaries of the body. The TDX is expressed as follows:

$$TDX = tan^{-1}\left(\frac{THG}{\left|\frac{\partial F}{\partial z}\right|}\right) \quad (5)$$

- ***Hyperbolic tilt angle (HTA)***

Another filter for enhancement of the edges is introduced by [16]. It called the hyperbolic tilt angle (HTA). The filter is given by:

$$HTA = R\left[tanh^{-1}\left(\frac{\frac{\partial F}{\partial z}}{THG}\right)\right] \quad (6)$$

where R denotes the real component of the hyperbolic tangent function.

- ***Gudermannian function (GF) technique***

It was introduced the Gudermannian function (GF) technique also called hyperbolic domain technique [21]. This technique uses the GF and the second derivative of the field. The GF is defined by:

$$GF = 2tan^{-1}\left\{tanh\left[2\left(-M + \frac{\frac{\partial HHG}{\partial z}}{\sqrt{\left(\frac{\partial HHG}{\partial x}\right)^2 + \left(\frac{\partial HHG}{\partial y}\right)^2}}\right)\right]\right\} \quad (7)$$

where:

$$HHG = \left|\left(\frac{\partial^2 F}{\partial x \partial z}\right)^2 + \left(\frac{\partial^2 F}{\partial y \partial z}\right)^2\right| \quad (8)$$

$\frac{\partial^2 F}{\partial x \partial z}$ and $\frac{\partial^2 F}{\partial y \partial z}$ represent the horizontal gradients along z.

The parameter M varies between 0.5 and 8, and its determination is left to the discretion of the interpreter [27]. In fact, the lowest value of M offers the best edge detection. The highest value increases resolution but risks eliminating edges. However, in general, the different values have little impact on the results and only change the resolution. The drawback of this technique lies in the use of higher-order derivatives, which can lead to an imprecise and incomplete plotting of the limits of anomalies.

- ***Modified Gudermannian Function Technique (MGTHG)***

It is an advanced, high-resolution filter that uses the modified Gudermannian function [52] to delineate the horizontal contours of potential field sources at different depths [27]. The MGTHG function improves the accuracy of boundary detection by refining the resolution of potential field data. It plays a crucial role in several existing filters, including the TA filter [14], the TDX filter [16], the TAHG filter [51], and the GF filter [48]. The MGTHG method is mainly based on the research conducted by [51]. The filter is defined as follows:

$$MGTHG = \frac{2}{\pi}tan^{-1}\left\{sinh\left[\frac{\frac{\partial THG}{\partial z} + \frac{\partial THG}{\partial z} - \sqrt{\left(\frac{\partial THG}{\partial x}\right)^2 + \left(\frac{\partial THG}{\partial y}\right)^2}}{\sqrt{\left(\frac{\partial THG}{\partial x}\right)^2 + \left(\frac{\partial THG}{\partial y}\right)^2}}\right]\right\} \quad (9)$$

The MGTHG filter allows the identification of regions with abrupt density variations. Its peaks effectively delimit the limits of structures [27]. Contrary to many new filters, the resolution of MGTHG results remains constant and does not depend on user-selected parameters [21, 27, 47, 48, 53-56]. A major advantage of the MGTHG filter is its ability to define boundaries with precision and clearness. Figure 3 shows the flowchart used to map the different lineaments of the study area.

4. Results and discussion

4.1. Results

- ***Bouguer anomaly map obtained from the combining terrestrial and EGM2008 gravity data***

The densified database allowed us to have the Bouguer anomaly map (Figure 4). This map shows a first negative anomalies zone located at the north of the study area, constituted of a vast domain of low gravity (–60 mGal). These anomalies could suggest a sedimentary infill, such as a lake basin where rivers have brought their alluvium, while volcanoes have spreading lava flows. This may be due either to the collapse of a sedimentary block or to the local thickening of a sedimentary series generated by the subsidence of the basement roof. In the South of Lere, West of Lame, we observe a negative anomalies zone (60 mGal), which could be due to sedimentary deposits in this area. This map also shows a positive anomalies area that extends from Bibémi to Lere in Chad and includes the Mayo Oulo-Lere sedimentary basin. The amplitude of these anomalies goes beyond 10 mGal.

For a good interpretation of anomalies, it is advisable to have the residual anomaly map which reflects the effects of the superficial structures. It was showed [39] from the method of [57] that degree 4 is the best degree of separation of Bouguer anomaly in the study area. For this purpose, in this study, the polynomial of degree 4 was used to separate the Bouguer anomaly into regional and residual.

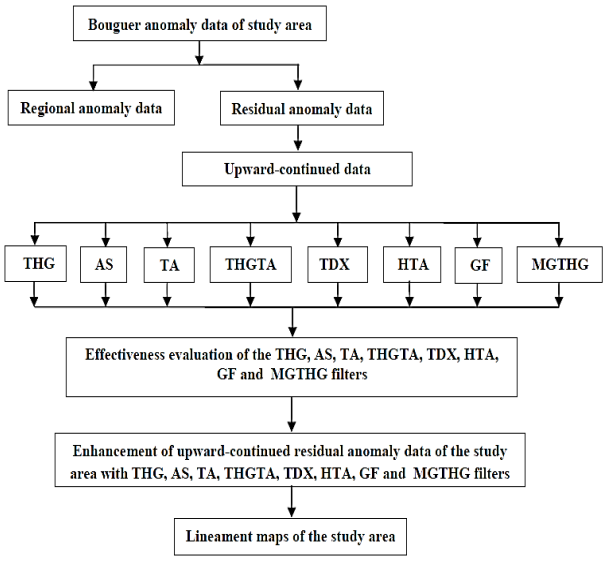

Figure 3: Flowchart for mapping the structural lineaments of the study area.

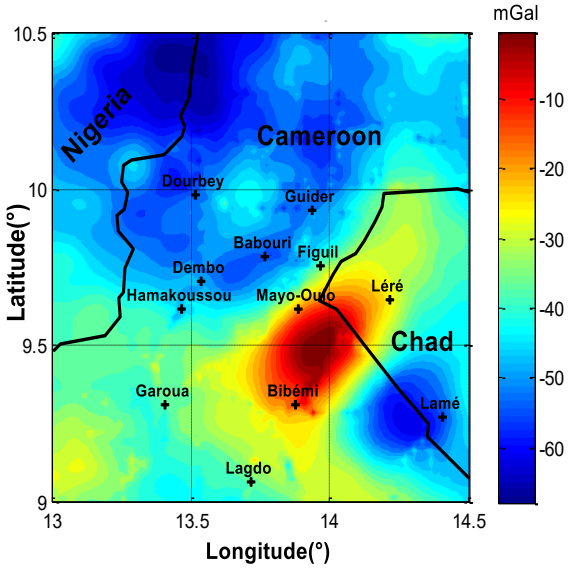

Figure 4. Bouguer anomaly map of the study area, obtained after combining terrestrial and EGM2008 gravity data.

- ***Residual anomaly map***

The residual anomaly map presented in Figure 5 shows the positive and negative areas. The first positive anomalies zone is located at the NW of the study area in the north of Dourbey. The anomalies values are between 0 and 10 mGal. This would be due to the presence of high density rocks within low density granitoid rocks. This map also shows another positive anomalies area that extends from Bibémi to Lere in Chad and includes the Mayo Oulo-Lere sedimentary basin. Their values reach 25 mGal. These anomalies show that the Mayo Oulo-Lere basin does not have the morphology of a sedimentary basin. It would therefore rather be a lake basin with dense rocks, probably basaltic. The second zone consists of negative anomalies. They are located in the south of Dourbey and around Dembo, Guider, where the Babouri-Figuil sedimentary basin is located. The values of these anomalies are between –15 and –5 mGal. This beach could correspond to the sedimentary deposits of the Babouri-Figuil basin. The map also shows another negative area located in the south of Lere, near the Cameroonian border. In this area, the anomalies values reaches –25 mGal. This would indicate the presence of weak formations relative to surrounding formations. Another negative anomaly zone is observed to the south of the study area that extends from Garoua to Lagdo. This zone, mainly made up of sandstone, would be linked to the Benue Trench. This map shows two areas of significant gradients characterized by a narrowing of the isoanomalous lines. The first is located between the localities of Bibémi, Lere and Lame and the second covers the localities of Mayo Oulo and Figuil. These gradient areas could be fracture zones.

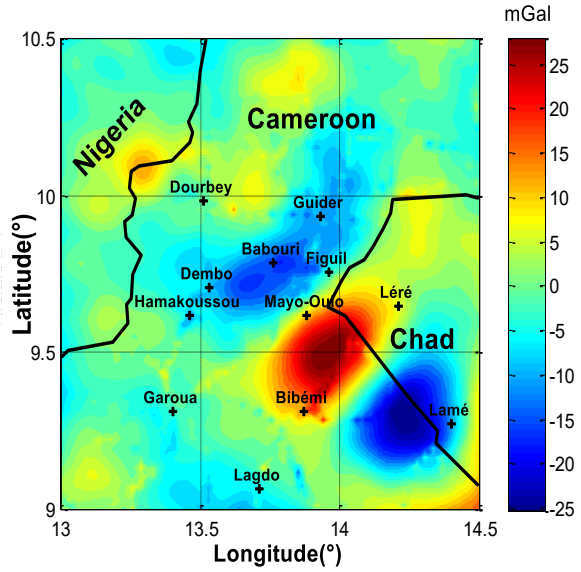

Figure 5. Map of the residual anomaly of degree 4 of the study area, obtained after combining terrestrial and EGM2008 gravity data.

- ***Residual anomaly map upward-continued to 300m***

As real gravity data usually contain noise, to apply the edge delimitation techniques based on derivatives, it is recommended to use an upward continuation filter to reduce the effects of noise. The choice of depth for this upward continuation depends on the geological information and the depth of the structures to be highlighted. Although depth values between 100 and 500 m do not show a significant difference, we opted for the median value (300 m) for our data. Figure 6 shows the residual anomaly map of the study area after upward continuation of 300 m.

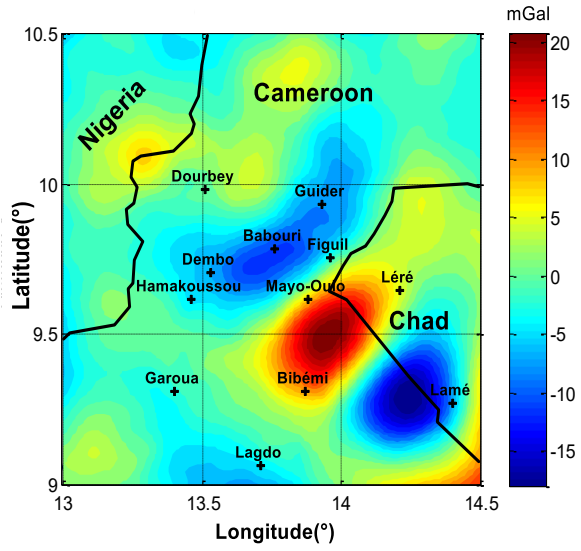

Figure 6: Residual anomaly map of the study area after upward continuation of 300 m.

The effectiveness and relevance of the MGTHG filter used in this work, as well as that of other edge detection filters such as: AS, THG, TA, THGTA, TDX, HTA, GF are evaluated by analyzing the results obtained during their application on gravity data of our study area.

- ***Edge delimitation maps of the structures***

Figures 7 a), b), c), d), e), f), g) and h) show the edge delimitation maps of the structures of the study area obtained using the filters AS, THG, TA, THGTA, TDX, HTA, GF and MGTHG respectively to the residual gravity anomaly upward-continued to 300 m.

Figures 7a) and b) illustrate the edge maps obtained from the AS and THG filters respectively. As can be seen, these maps are dominated by the responses of large amplitude anomalies originating from shallow sources located in the southeastern part of the area. However, the edges of the lower amplitude anomalies cannot be determined. Therefore, the AS and THG filter maps cannot clearly show the edges of the deep geological sources; this makes it difficult to realize a definitive structural map of the study area.

Figure 7c) shows the edge images created by the TA filter. Although this filter provides a balanced representation of the anomaly sources, it does not provide precise boundaries for the geological features of the region. The edge image created by the THGTA filter shown in Figure 7d) does not present a balanced representation of the distribution of the different sources. Figure 7e) shows the results of the TDX filter. Although the latter is more effective than the AS, THG, TA and THGTA filters in generating distinct contour images, the source contours appear interconnected, thus complicating the interpretation of the geological features of the region. Figure 7f) illustrates the results of edge detection using the HTA filter. This image shows that this filter cannot effectively delineate all the edges of the geological structures. Figure 7g) presents the results obtained by applying the GF filter taking a value of M=0.5. Several values of M were tested, the value of 0.5 was chosen because it best represents the contours of the structures. As we can see, in this figure, the delimitation of the edges of the structures of the region appears blurred and indistinct. Figure 7h) illustrates the edges identified by the MGTHG filter. On this map, the edges of the significant amplitude anomalies as well as those of the low amplitude anomalies are visible. This image shows that this filter has a higher resolution in delineating the edges compared to the other filters presented. The MGTHG filter thus allows us to successfully identify the lineaments and therefore generate a structural map of the study area.

Figure 8 shows the gravity lineament map of the study area extracted by applying the MGTHG filter. It presents more lineaments in the northern and southern part of the area than in the center. This map shows that most of the structural features determined in the study area are oriented in the WSW-ENE, NE-SW, E-W and NNW-SSE directions. Important lineaments such as the one passing through Mayo Oulo and Figuil, Garoua and Lagdo are visible on this map (Figure 8). These directions could be associated to those of the major tectonic and hydrogeological structures in the area such as the Cameroon volcanic line, the Benue Trough, the Mayo Kébi and the Benue River. Important lineaments such as the one passing through the localities of Mayo-oulo and Figuil, Garoua and Lagdo are visible on this map. They could be associated with the two branches of the Cameroon volcanic line. From a geological point of view, these lineaments could also be linked to the volcanic activities that led to the appearance of volcanic materials on the surface.

4.2. Discussion

A comparative study between the structure edge map obtained by applying the MGTHG filter to the gravity data of the area and those obtained by other commonly used filters including AS, TG, TA, THGTA, TDX, HTA and GF was made (Figure 7). The results of this comparison show clearly that the MGTHG filter is less dependent on the depth of the sources, it can not only generate edges of the sources of significant amplitude anomalies but also those of the sources of low amplitude anomalies, whereas the AS, THG and THGTA filters place much more emphasis on shallow geological features with relatively

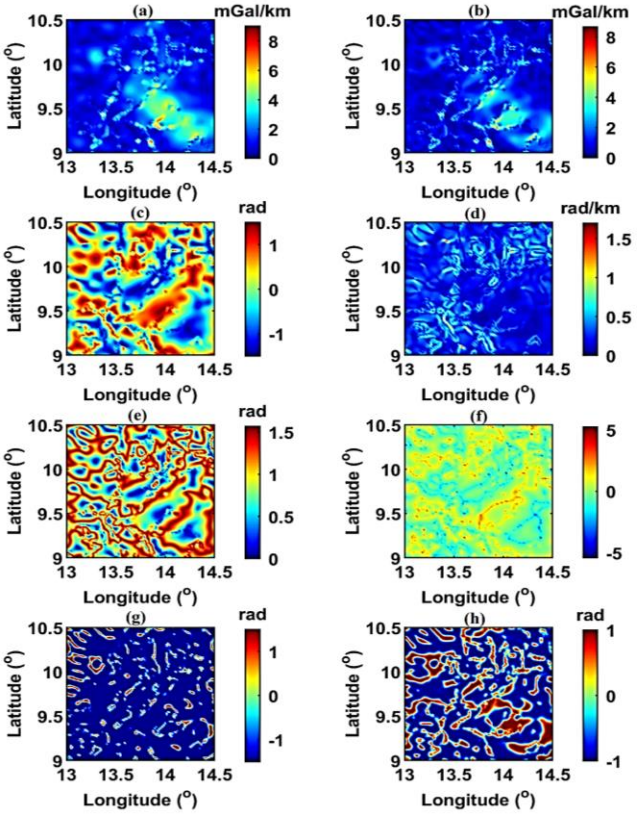

Figure 7. Map of: a) AS; b) THG; c) TA; d) THGTA; e) TDX; f) HTA; g) GF and h) MGTHG.

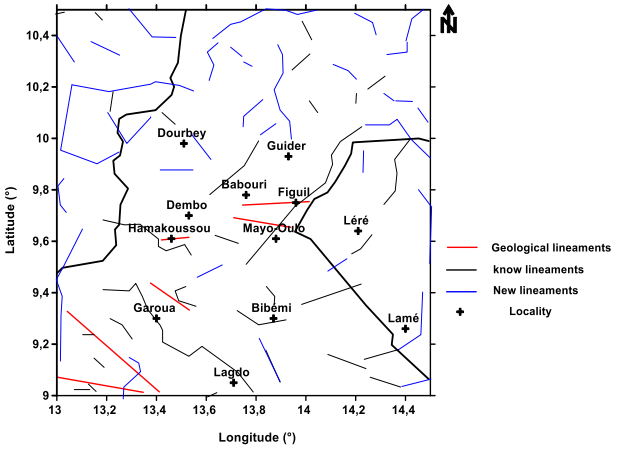

Figure 8. Structural map of the study area obtained from the MGTHG filter.

short wavelengths. The MGTHG filter is better than the TA, TDX and HTA filters because it delineates the contours of geological structures more precisely, thus providing an improved interpretation. Furthermore, it does not generate false outlines, which can create misleading artifacts in the data and further complicate the interpretation process. The MGTHG filter provides a much clearer map of the structure outlines with a higher resolution than that presented by the GF filter, which is nevertheless more efficient than the other filters (AS, THG, TA, THGTA, TDX, HTA). This has made it possible to reveal the details of the structures and thus leads to a good interpretation. The MGTHG filter provides better results as it provides greater precision, clarity and good resolution compared to other filters. Thus, it provides an improved geological interpretation in terms of edge delineation. This

made it easier for us to create the structural map of the study area. The examination of this map generally indicates that there is a good correlation between the lineaments present on this map and the existing geological and tectonic structures in the study area (Figure 8). This map confirms the presence of lineaments previously detected using edge detection methods applied to potential field data, which have proven very effective [58-60] (Figure 8). However, it also presents new, previously unknown lineaments (Figure 8).

Analysis of the trends of the mapped lineaments showed a strong correlation between the directions of the lineaments extracted in this work (WSW-ENE, NE-SW, E-W and NNW-SSE) and those of the existing geological lineaments and those mapped by [37, 59-64] in the study area. These trends are also consistent with those of the major tectonic and hydrogeological structures of the area (Cameroon Volcanic Line, Benue Trough, Mayo Kebi and Benue River).

5. Conclusion

In this work, the modified Gudermannian function filter was applied to gravity data to extract lineaments in the crust of the Babouri-Figuil and Mayo Oulo-Lere sedimentary basins, (northern Cameroon and southern Chad). The results obtained from the interpretation of the maps show that the MGTHG filter, compared to others filters, can provide more precise and clearer images of the boundaries of geological structures.

These results also show that most of the lineaments detected in the study area are oriented in the WSW-ENE, NE-SW, E-W and NNW-SSE directions. Important lineaments such as the one passing through Mayo Oulo and Figuil, Garoua and Lagdo have been highlighted. These results provide a new structural map of these two sedimentary basins as well as the surrounding area. The results of this work thus increase the structural knowledge of the area. This knowledge can be used for the selection of sites for exploration of groundwater and underground mineral sources, as well as for the assessment of environmental risks during the implementation of major public works in the area

Acknowledgements

The authors sincerely thank to International Gravimetric Bureau (IGB) for data used in this work.

Funding

No funding was received to assist with the preparation of this manuscript.

Conflict of interest

The authors have no conflicts of interest to declare that are relevant to the content of this article.

Data availability statement

The corresponding author guarantees the availability of the data used to carry out this study.

Contributions of authors

Saidou Bouba, Nlen wounle Barnabas and Yaya and Nguilaye Salomon contributed to the article writing.

Bouba Apollinaire and Oyoa Valentin contributed to establish the basic of the article and to its scientific development.

Mohamadou Alidou contributed to the scientific development of the article.

References

[1]. Pham, L.T., Eldosouky, A.M., Oksum, E., Saada, S.A. (2020a). A new high resolution filter for source edge detection of potential field data. Geocarto International, 1-18. Doi: 10.1080/10106049.2020.1849414.

[2]. Oksum, E., Le, D.V., Vu, M.D., Nguyen, T.H.T., Pham, L.T. (2021). A novel approach based on the fast sigmoid function for interpretation of potential field data. Bulletin of Geophysics and Oceanography, 62(3): 543-556. https://doi.org/10.4430/bgta0348

[3]. Eldosouky, A.M., Pham, L.T., and Henaish, A. (2022). High precision structural mapping using edge filters of potential field and remote sensing data: a case study from Wadi Umm Ghalqa area, south eastern Desert, Egypt. Egypt. J. Remote Sens. Space Sci., 25, 501-513, doi: 10.1016/j.ejrs.2022.03.001.

[4]. Kafadar, O. (2017). CURVGRAV-GUI : a graphical user interface to interpret gravity data using curvature technique. Earth Sci. Inf., 10, 525-537.

[5]. Pham, L.T., Do, T.D., Oksum, E. (2018). A new method for edge detection in interpretation of potential feld data. Journal of Engineering Sciences and Design, 6(4), 637-642.

[6]. Oksum, E., Dolmaz, M.N., Pham, L.T. (2019). Inverting gravity anomalies over the Burdur sedimentary basin, SW Turkey. Acta Geod. Geophys., 54, 445-460.

[7]. Eldosouky, A.M., Pham, L.T., Mohammed, H., Pradhan, B. (2020). A comparative study of THG, AS, TA, Theta, TDX and LTHG techniques for improving source boundaries detection of magnetic data using synthetic models : a case study from G. Um Monqul, north Eastern Desert, Egypt. J. Afr. Earth Sci., 170, 103940.

[8]. Cordell. L., and Grauch, V.J.S. (1985). Mapping basement magnetization zones from aeromagnetic data in the San Juan basin, New Mexico. In: Hinze W.J. (ed), The utility of regional gravity and magnetic maps. Publ. Soc. Explor. Geophys., 181-197, doi: 10.1190/1.0931830346.ch16.

[9]. Roest, W.R., Verhoef, J., and Pilkington, M. (1992). Magnetic interpretation using the 3 D analytic signal. Geophys., 57, 116-125.

[10]. Fedi, M., Florio, G. (2001). Detection of potential fields source boundaries by enhanced horizontal derivative method. Geophys Prospect., 49, 40-58.

[11]. Nasuti, Y., Nasuti, A., Moghadas, D. (2019). STDR: a novel approach for enhancing and edge detection of potential field data. Pure Appl Geophys., 176(2), 827-841.

[12]. Tatchum, C.N., Tabod, T.C., Koumetio, F., Manguelle-Dicoum, E. (2011). A Gravity Model Study for Differentiating Vertical and Dipping Geological Contacts with Application to a Bouguer Gravity Anomali Over the Foumban Shear Zone, Cameroon. Geophysica, 47(1-2), 43-55.

[13]. Pham, L.T., Oksum, E., Le, D.V., Ferreira, F.J.F., Le, S.T. (2021). Edge detection of potential field sources using the softsign function. Geocarto International, 1-14. Doi: 10.1080/10106049.2021.1882007.

[14]. Miller, H.G., and Singh, V. (1994). Potential field tilt a new concept for location of potential field sources. J. Appl. Geophys., 32, 213-217, doi: 10.1016/0926-9851(94)90022-1.

[15]. Verduzco, B., Fairhead, J.D., Green, C.M. and MacKenzie, C. (2004). New insights into magnetic derivatives for structural mapping. Lead. Edge, 23, 116-119.

[16]. Cooper, G.R.J., and Cowan, D.R. (2006). Enhancing potential

field data using filters based on the local phase. Comput. Geosci., 32, 1585-1591.

[17]. Deniz Toktay H., Aydogan D., and Yüksel F. (2021a). Quantitative analysis of total magnetic anomaly maps on archaeological sites - Part 1. Math. Methods Appl. Sci., 44, 13696-13710.

[18]. Deniz Toktay H., Aydogan D., and Yüksel F. (2021b). Quantitative analysis of total magnetic anomaly maps on archaeological sites - Part 2. Math. Methods Appl. Sci., 44, 13684-13695.

[19]. Eldosouky A.M., El-Qassas R.A.Y., Pour A.B., Mohamed H., and Sekandari M. (2021). Integration of ASTER satellite imagery and 3D inversion of aeromagnetic data for deep mineral exploration. Adv. Space Res., 68, 3641- 3662.

[20]. Pham, L.T., and Prasad K.N.D. (2023). Analysis of gravity data for extracting structural features of the northern region of the central Indian Ridge. Vietnam J. Earth Sci., 45, 147-163, doi: 10.15625/2615-9783/18206.

[21]. Alvandi, A., Su, K., Ai, H., Ardestani, V.E., and Lyu. C. (2023a). Enhancement of potential field source boundaries using the hyperbolic domain (Gudermannian function). Miner., 13, 1312, doi: 10.3390/min13101312.

[22]. Ai H., Ekinci Y.L., Alvandi A., Deniz Toktay H., Balkaya Ç. and Roy, A. (2024a). Detecting edges of geologic sources from gravity or magnetic anomalies through a novel algorithm based on hyperbolic tangent function, Turkish Journal of Earth Sciences, 33(6). https://doi.org/10.55730/1300-0985.1936

[23]. Ai, H., Deniz Toktay, H., Alvandi, A., Pasteka, R., Su, K., and Liu, Q. (2024b). Advancing potential field data analysis: the Modified Horizontal Gradient Amplitude method (MHGA). Contributions to Geophysics and Geodesy, 54(2), 119-143. https://doi.org/10.31577/congeo.2024.54.2.1

[24]. Alvandi, A., Ardestani, V. E., and Motavalli-Anbaran, S.H. (2024). Novel Detectors Based on the Elliott Function for Mapping Potential Field Data: Application to Aeromagnetic Data from Indiana, United States. Annals of Geophysics, 67(6), GP656. https://doi.org/10.4401/ag-9146

[25]. Deniz Toktay, H., Prasad, K.N.D., and Alvandi, A. (2024). Edge enhancement of potential field data using the Enhanced Gradient (EG) filter. Bull. Miner. Res. Explor., 174, 55-66, doi: 10.19111/bulletinofmre.1386653.

[26]. Alvandi, A., Toktay, H.D., and Pham, L. (2022). Capability of improved Logistics filter in determining lateral boundaries and edges of gravity and magnetic anomalies Tuzolu Area Turkey, Journal of Mining Engineering, 17(56), 57-72 doi:10.22035/ijme.2022.538985.1889

[27]. Alvandi, A., Ardestani, V. E., and Motavalli-Anbaran, S. H. (2025). Enhancement of the total horizontal gradient of potential field data using the Modified Gudermannian Function (MGTHG): application to aeromagnetic data from Georgia, USA. Bulletin of Geophysics and Oceanography, 66(1), 73-94. http://dx.doi.org/10.4430/bgo00479

[28]. Ntsama Atangana, J.A. (2013). Magnetostratigraphy and sedimentology of the Cretaceous formations of the Hamakoussou and Mayo Oulo-Lere sedimen¬tary basins in North Cameroon (Benue trough) [Ph.D. thesis]. Poitiers: University of Poitiers. (in French).

[29]. Ngako, V., Jegouzo, P., Soba, D. (1989). Deformation and metamorphism in the Pan-African Poli chain (Northern-Cameroon): Geodynamic and paleo¬geographic implications. Journal of African Earth Sciences. 9, 541–555. (in French).

[30]. Guiraud, R., Maurin, J.C. (1991). Rifting in Africa in the Lower Cretaceous: Structural synthesis, demonstration of two stages in the genesis of the basins, relationships with peri-African ocean¬ic openings. Report of the Geological Society of France. 162(5), 811–823. (in French). DOI: https://doi.org/10.2113/gssgfbull.162.5.811

[31]. Ndjeng, E. (1992). Studies of the sedimentation and geodynamic model of two Lower Cretaceous basins of Cameroon: Babouri-Figuil and Mayo Oulo-Lere [Ph.D. thesis]. Yaounde: University of Yaounde. (in French).

[32]. Gèze, B. (1941). On the volcanic Massifs of Western Cameroon. Report of Academic Sciences of Paris. 212, 498–500. (in French).

[33]. Bessong, M. (2012). Paleoenvironments and dia¬genesis in a Cretaceous sandstone reservoir of the Benue trough in North Cameroon: The Garoua sandstone [Ph.D. thesis]. Poitiers: University of Poitiers. (in French).

[34]. Abate Essi, J.M., Marcel, J., Diab, D.A., et al. (2019). Gravity modeling of the Au-U mineralized crust at the North-Central Cameroon illustrating crutal permeability. Natural Resources Research. 29, 473–497. DOI: https://doi.org/10.1007/s11053-019-09506-4

[35]. Abubakar, A.J., Hashim, M., Beiranvand, A.P. (2018). Identification of hydrothermal alteration minerals associated with geothermal system using ASTER and Hyperion satellite data: A case study from Yankari Park, NE Nigeria, Geocarto International. 34(6), 597–625. DOI: https://doi.org/10.1080/10106049.2017.142 1716

[36]. Eyike, A., Werner, S.C., Ebbing, J., et al. (2010). On the use of global potential field models for region¬al interpretation of the west and central African rift system. Tectonophysics. 492(1–4), 25–39.

[37]. Abate Essi, J.M., Marcel, J., Yene Atangana, J.Q., et al. (2017). Interpretation of gravity data derived from the Earth Gravitational Model EGM2008 in the Center–North Cameroon: Structural and min¬ing implications. Arabian Journal of Geosciences. 10, 130. DOI: http://doi.org/10.1007/s12517-017-2919-y

[38]. Bouba, A., Kamguia, J., Tabod, C.T., et al. (2017). Sub¬surface Structural Mapping Using Combined Ter¬restrial and Grace Gravity Data of the Adamawa Plateau (North Cameroon). International Journal of Geosciences. 8(7), 869–887. DOI: https://doi.org/10.4236/ijg.2017.87050

[39]. Saidou, B., Bouba, A., Oyoa, V., et al. (2024). Crustal Structures Inferred from Combined Terrestrial and Earth Gravity Data beneath the Babouri-Figuil and Mayo Oulo Lere Basins, North Cameroon and South Chad. Earth and Planetary Science. 3(1): 21–34. DOI: https://doi. org/10.36956/eps.v3i1.928

[40]. Collignon, F. (1968). Gravimetry of the recognition of the Republic of Cameroon, ORSTOM. (in French).

[41]. Louis, P. (1970). Geophysical contribution to the knowledge of the Lake Chad basin. OSTROM Mem¬ory: Paris. (in French).

[42]. Poudjom-Djomani, Y.H., Diament, M., Wilson, M. (1997). Lithospheric structure across the Adamawa plateau (Cameroon) from gravity studies. Tectono¬physics. 273(3–4), 317– 327. DOI: https://doi.org/10.1016/S0040-1951(96) 00280-6

[43]. Yushan, Y., Yuanyuan L. (2017). Crustal structure of the Dabie orogenic belt (eastern China) inferred from gravity and magnetic data. Tectonophysics. 17:1–17.

[44]. Marcel, J., Abate Essi, J.M., Njandjock, N.P., Meli, I.L., Mahamat, A., Manguelle- Dicoum, E. (2018). Geodynamic insights of the

Cameroon Volcanic Line (Western Africa) from isostatic gravity anomalies. J Geodyn., 121, 36-48.

[45]. Pavlis, N.K., Holmes, S.A., Kenyon, S.C., et al. (2012). The development and evaluation of the Earth Gravitational Model 2008 (EGM2008). Journal of Geophysical Research. 117(B4). DOI: https://doi.org/10.1029/2011JB008916

[46]. Saibi, H., Aboud, E., and Ehara, S. (2012). Analysis and interpretation of gravity data from the Aluto-Langano geothermal field of Ethiopia. Acta Geophys., 60, 318-336.

[47]. Prasad, K.N.D., Pham, L.T., Singh, A.P., Eldosouky, A.M., Abdelrahman, K., Fnais, M.S., and Gómez-Ortiz, D. (2022a). A novel Enhanced Total Gradient (ETG) for interpretation of magnetic data. Miner., 12, 1468, doi: 10.3390/ min12111468.

[48]. Prasad, K.N.D., Pham, L.T., and Singh, A.P. (2022b). A novel filter "ImpTAHG" for edge detection and a case study from Cambay Rift basin, India. Pure Appl. Geophys., 179, 2351-2364.

[49]. Pham, L.T., Oksum, E., Do, T.D., and Vu, M.D. (2020b). Comparison of different approaches of computing the tilt angle of the total horizontal gradient and tilt angle of the analytic signal amplitude for detecting source edges. Bull. Mineral Res. Explor., 163, 17, doi: 10.19111/bulletinofmre.746858.

[50]. Eldosouky, A.M., and Saada, S.A. (2020). Source edge detection (SED) of aeromagnetic data: synthetic examples and a case study from Haimur area, south Eastern Desert, Egypt. Arabian J. Geosci., 13, 1-12.

[51]. Ferreira, F.J.F., de Souza, J., Bongiolo, A.B.S., and de Castro, L.G. (2013). Enhancement of the total horizontal gradient of magnetic anomalies using the tilt angle. Geophys., 78, J33-J41.

[52]. Nayak, A.K., and Pal, A. (2019). Development and validation of an adsorption kinetic model at solid-liquid interface using normalized Gudermannian function. J. Mol. Liq., 276, 67-77.

[53]. Alvandi, A., Toktay, H., and Ardestani, V.E. (2023b). Edge detection of geological structures based on a logistic function: a case study for gravity data of the western Carpathians. Int. J. Min. Geo-Eng., 57, 267-274, doi: 10.22059/ijmge.2023.353516.595018.

[54]. Alvandi, A., and Ardestani, V.E. (2023c). Edge detection of potential field anomalies using the Gompertz function as a high-resolution edge enhancement filter. Bull. Geophys. Ocean., 64, 279-300.

[55]. Ibraheem, I.M., Tezkan, B., Ghazala, H., and Othman, A.A. (2023). A new edge enhancement filter for the interpretation of magnetic field data. Pure Appl. Geophys., 180, 2223-2240.

[56]. Pham, L.T. (2023). A novel approach for enhancing potential fields: application to aeromagnetic data of the Tuangiao, Vietnam. Eur. Phys. J. Plus., 138, 1134, doi: 10.1140/epjp/s13360-023-04760-1.

[57]. Zeng, H., Xu, D., Tan, H. (2007). A model study for estimating optimum upward continuation height for gravity separation with application to a Bou¬guer gravity anomaly over a mineral deposit, Jilin province, northeast China. Geophysics. 72(4), 145–150.

[58]. Nlen wounle, B.Y., Oyoa, V., Gouet, D.H., Ekoro, N.H.L., Njandjock, N.P., Doka, Y.S. (2022). Structural study of the transition zone between the Benue and Lake Chad Basins (Central Africa) using gravity data. Geocarto International, DOI: 10.1080/10106049.2022.2120636

[59]. Bouba, A., Njeudjang, K., Aime, M.J., Raouf, A., Ghomsi, F.E.K., Pham, L.T. (2024). Analyzing Structural Lineaments in the Garoua Sedimentary Basin via SGGUGM-2 Gravity Data: Enhanced edge-detection techniques. Environmental and Earth Sciences Research Journal. 11(2), 28-35. https://doi.org/10.18280/eesrj.110201

[60]. Kamto, P.G., Oksum, E., Yap, L. et al. (2024). High precision structural mapping using advanced gravity processing methods: a case study from the North region of Cameroon. Acta Geophys. 72, 2263-2280.https://doi.org/10.1007/s11600-023-01211-4

[61]. Mouzong, M.P., Kamguia, J., Nguiya, S., Shandini, Y., Manguelle- Dicoum, E. (2014). Geometrical and structural characterization of garoua sedimentary basin, Benue trough, North Cameroon, using gravity data. J Biol and Earth Sciences. 4 (1):25-33.

[62]. Fofie, K.A.D., Koumetio, F., Kenfack, J.V., Yemele, D. (2019). Lineament characteristics using gravity data in the Garoua Zone, North Cameroon: natural risks implications. Earth Planet Phys. 3(1), 33-44.

[63]. Ghomsi, F.E.K., Pham, L.T., Steffen, R., Ribeiro-Filho, N., Tenzer, R. (2022). Delineating structural features of North Cameeroon using the EIGEN6C4 high-resolution global gravitational model. Geol J. 57(10), 4285-4299.

[64]. Nlen wounle, B.Y., Oyoa, V., Njandjock, N.P., Doka, Y.S. (2023). A new MATLAB code for locating lineaments in the earth's crust from gravity data-a case of the transition zone between Benue basin and Lake Chad basin: cameroon. Arab J Geosci. 16(12). doi: 10.1007/s12517-023- 11797-0.